*Res Mechanica* **1** (1980) 85–99

# NUMERICAL EXPERIMENTS IN FINITE ELEMENT ANALYSIS OF THERMOELASTOPLASTIC BEHAVIOUR OF MATERIALS. FURTHER DEVELOPMENTS OF THE PLASTEF CODE

F. G. BASOMBRÍO and G. SÁNCHEZ SARMIENTO

(*Centro Atómico Bariloche (Comisión Nacional de Energía Atómica), 8400 San C. de Bariloche, Argentina*

(Received: 23 June, 1979)

*ABSTRACT*

*In a previous paper the finite element code PLASTEF for the numerical simulation of thermoelastoplastic behaviour of materials was presented in its general outline. This code employs an initial stress incremental procedure for given histories of loads and temperature. It has been formulated for medium sized computers. The present work is an extension of the previous paper to consider additional aspects of the variable temperature case. Non-trivial tests of this type of situation are described. Finally, details are given of some concrete applications to the prediction of thermoelastoplastic collapse of nuclear fuel element cladding.*

## 1. INTRODUCTION

For the mechanical design of reactor components operating under severe conditions of pressure and temperature-gradient it is essential to know the inelastic responses of the structural parts for typical transients. In general such parts have a wide variety of geometrical forms.

As one of the stages of a program related to the numerical simulation of inelastic mechanical behaviour, the authors recently developed the code PLASTEF,[5] written for medium sized computers. Its purpose is to solve the incremental equations of thermoelastoplasticity (within the Levy–Mises–Prandtl–Reuss model), in two independent spacial variables[2,4] according to prescribed histories of loads and temperatures. These equations correspond to the hypothesis of small strains and displacements, which covers a large number of practical cases. The methods of Zienkiewicz and co-workers[1–3] were followed, using the initial stress procedure.



*Res Mechanica* 0143-0084/80/0001-0085/$02·25 

In contrast to the codes for solving well-established problems such as heat conduction, elasticity, etc., the elastoplastic codes are of considerably greater complexity. In ref. 5 the general ouline of the system PLASTEF was given, and relevant tests for the plane stress case, at constant temperature were described. The present paper complements the preceding one in that it considers variable temperature cases of plane stress and strain, including some solved examples and an application to a problem of nuclear reactor engineering.

## 2. DESCRIPTION OF THE CODES

In order to reduce the high speed memory requirements, and thus to enable it to be implemented on medium sized computers, the system PLASTEF is composed of the following four codes:

*Code PLASTEF1:* solves general elastoplastic problems for plane stresses or strains.

*Code PLASTEF2:* solves general thermoelastoplastic problems for plane stresses or strains. It also deals with any given history of imposed $\sigma_z$ stresses in a direction perpendicular to the plane of the two-dimensional system under study.

*Code PLASTEF3:* solves general elastoplastic problems for axisymmetric cases.

*Code PLASTEF4:* solves general thermoelastoplastic problems for axisymmetric cases.

Histories of loads, temperatures (incremental temperature distributions at each step) and $\sigma_z$ must previously be evaluated and stored in disks by the code PREPLASTEF. Decoupling of mechanical and thermal effects was assumed. This is a reasonable hypothesis within the general assumptions of the model.

The fundamental steps of the program are the following:

(a) Evaluate the first yield limit load (only for PLASTEF1 and 3).
(b) Evaluate incremental loads (PLASTEF1 and 3). Read from disks incremental loads, incremental temperature distributions (PLASTEF2 and 4) and incremental $\sigma_z$ (PLASTEF2).
(c) Solve the thermoelastic incremental problem with initial stresses.
(d) For each element make the corresponding adjustments: (1) if it just enters the plasticity state, and (2) for small departures from the yield surface.[5]
(e) Store residual stresses.
(f) If the residual stresses are not small enough, go to (c).

(g) Store incremental stresses, incremental plastic strains, incremental nodal displacements and incremental equivalent plastic strain.
(h) Print results of the load step $n$.
(i) If the histories of loads and temperatures are not concluded, go to (b).
(j) END.

For the solution of the linear algebraic system corresponding to the incremental thermoelastic problem, the factorisation method of Cholesky is employed.

The program uses triangular elements with linear interpolation functions, to cover a general plane domain which can also be multiply connected. It has a total high speed memory requirement of 100 kbytes and it also needs disk auxiliary storage. This capacity permits triangular nets of about 300 elements and 200 nodes. A problem of this size takes nearly 50 s for each iteration (steps (c) to (f)). (The programs were implemented on the IBM/360-Mod. 44 of the Centro de Cómputos, Centro Atómico Bariloche, CNEA.)

## 3. TEST EXAMPLE

The most relevant test example solved with the code and not described in ref. 5 is now briefly summarised.

For a thick-walled cylinder of the geometrical dimensions and thermoelastoplastic properties shown in Fig. 1, three different problems were solved. (1) Loading, unloading and reloading at a constant temperature $T = 21{\cdot}11\,°C$ (70 °F). (2) Variable imposed internal pressure and temperature according to the histories represented in Fig. 4, for the expansion coefficient $\alpha = 0$. (3) A

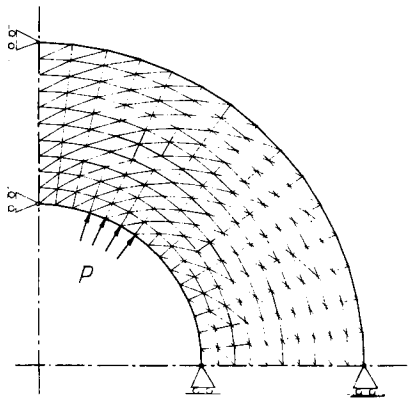


$E = 60.94\ kg/mm^2\ (86666\ lb/in^2)$
$G = 23.44\ kg/mm^2\ (33333\ lb/in^2)$
$\nu = 0.3$
$\alpha = 0$ y $\alpha = 1.666 \times 10^{-7}(°C)^{-1}\ (3 \times 10^{-7}(°F)^{-1})$

| T °C (°F) | Yield kg/mm² (lb/in²) |
|---|---|
| 21.11 (70) | 0.012 (17.32) |
| 37.78 (100) | 0.011 (15.26) |
| 93.33 (200) | 0.010 (13.88) |
| 148.89 (300) | 0.009 (12.72) |

Fig. 1. Geometrical dimensions and thermoelastoplastic properties of the thick-walled cylinder.

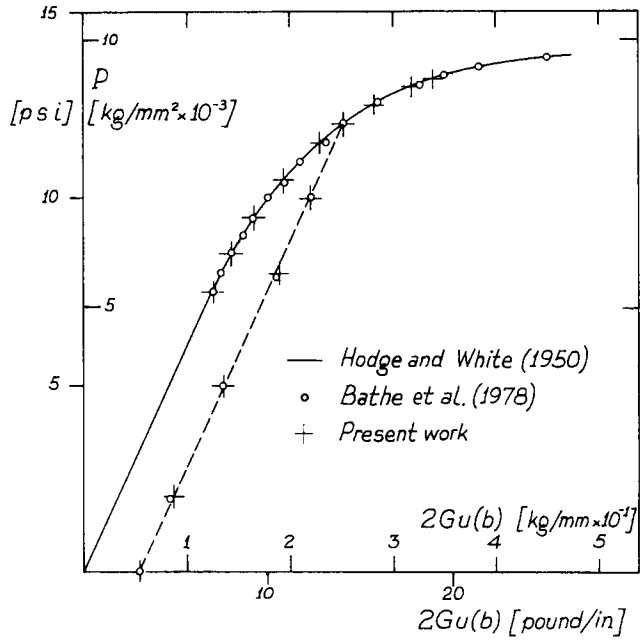


Fig. 2. Elastoplastic displacement response of the thick-walled cylinder.

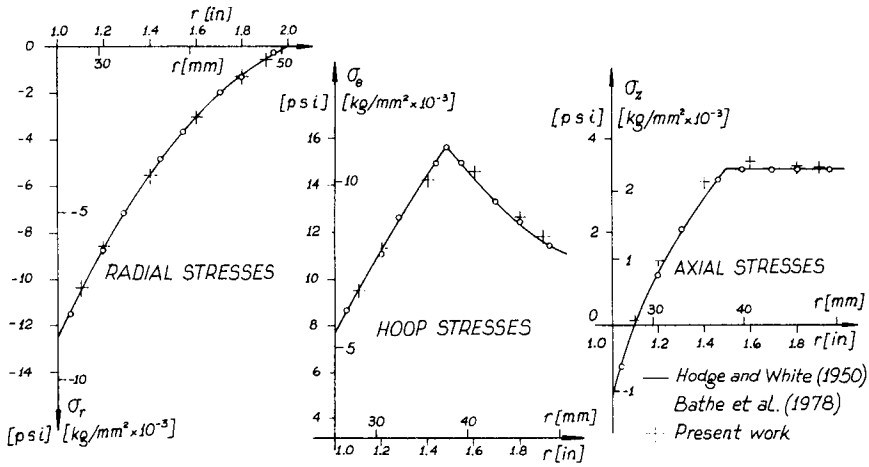


Fig. 3. Elastoplastic stress distribution through the thickness of the thick-walled cylinder at $p = 0{\cdot}879 \times 10^{-2}$ kg/mm$^2$ (12·5 psi).

similar case but with $\alpha = 1{\cdot}666 \times 10^{-7}$ $(°C)^{-1}$ $(3 \times 10^{-7}$ $(°F)^{-1})$. The first two situations were previously solved by Bathe *et al.*[6]

For the first problem the values $2Gu(b)$, proportional to the outer radial displacements $u(b)$, are plotted in Fig. 2 against the internal pressure $p$ and compared both with the solution of Hodge and White[9] and the results obtained by Bathe *et al.*[6] Figure 3 shows the stress graphs for $p = 0{\cdot}879 \times 10^{-2}$ kg/mm$^2$(12·5 lb/in$^2$), again compared with the previous results.

Figure 4 gives the histories of loads and temperatures corresponding to the second and third cases, the response value $2Gu(b)$ as a function of time for

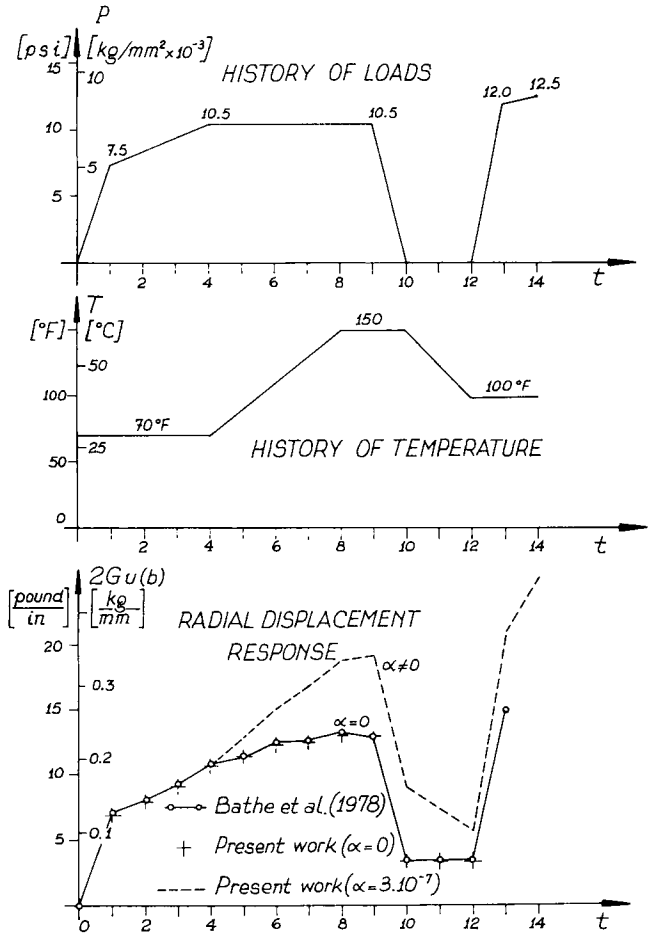


Fig. 4. Load and temperature histories, and thermoelastoplastic displacement response of the thick-walled cylinder.

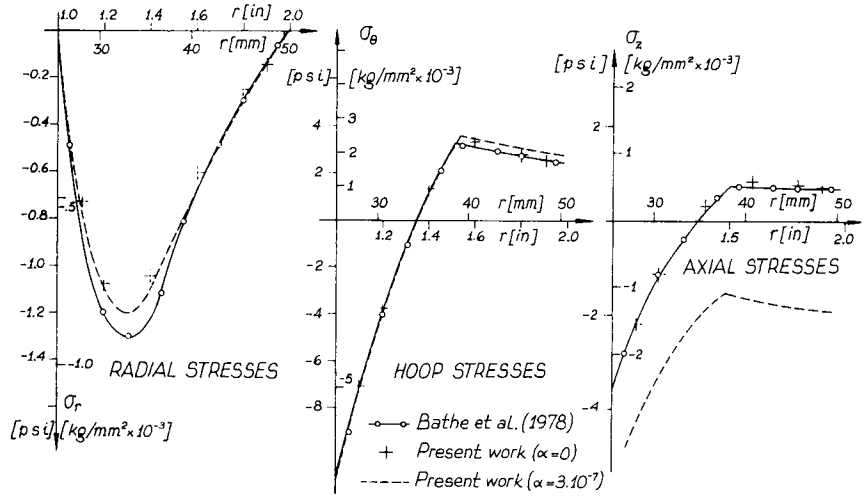


Fig. 5. Residual stress distribution of the thick-walled cylinder at $t = 10$.

$\alpha = 0$ (Fig. 4) compared with the results of ref. 6 and the similar response for the third case in which $\alpha = 1{\cdot}666 \times 10^{-7}$ $(°C)^{-1}$ $(3 \times 10^{-7}$ $(°F)^{-1})$.

Finally in Fig. 5 the residual stresses at $t = 10$ $(p = 0)$ for $\alpha = 0$ and $\alpha = 1{\cdot}666 \times 10^{-7}$ $(°C)^{-1}$ are compared with those given in ref. 6 when $\alpha = 0$.

A satisfactory agreement is always observed except perhaps for the radial stress in Fig. 5. For $\alpha \neq 0$ the external displacement response is seen to be in accord with expectations.

## 4. APPLICATION TO NUCLEAR FUEL CLADDING MODELLING

### 4.1. *Formulation of the problem*

The fuel element cladding of some nuclear power reactors has welded onto it a set of slider ribs (see Fig. 6) of the same material. These ribs can slide longitudinally on the corresponding fuel element separator's supports, so as to permit the free differential expansion (in the longitudinal direction) of the different rods that constitute the fuel element.

This zone of the cladding is perhaps the one which differs most from the geometrical hypothesis of the one-dimensional computer codes generally used to simulate numerically the thermomechanical behaviour of fuel rods subjected to in-reactor conditions. With this hypothesis the rod must be idealised as axially symmetric and infinite in its longitudinal direction. For the application of those codes to the whole rod, it is therefore of fundamental importance to know the extent to which the final resistance of the cladding is modified by incorporating the ribs.

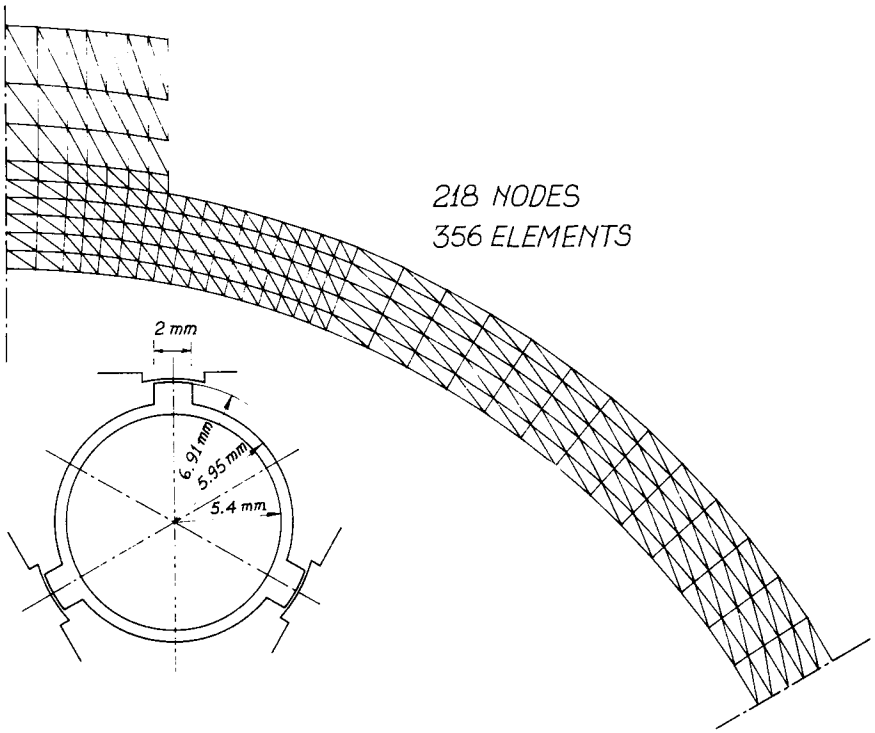


Fig. 6. The reactor cladding at the rib zone and the finite element mesh.

With this purpose in mind, an analysis of the thermoelastoplastic behaviour of a specific reactor cladding (of Zircaloy-4) has been made for realistic pressure and thermal conditions. A general outline of this analysis is given below. Details of the calculations and additional information can be found in ref. 7.

4.2. *Situations analysed, hypothesis and data*

A two-dimensional representation (with plane symmetry) of the real geometry was considered.

Only two limiting cases have been studied:

(i) The initial gap (see Fig. 6) between the ribs and the separator's supports vanishes at the final stage of the manufacturing, that is, when the rod has an inner pressure of 17 atmospheres, its external pressure is 1 atmosphere and it is at a temperature of 20 °C.

(ii) This initial gap is sufficiently large so as to remain open at any stage of the calculations, i.e. the presence of the separator is ignored.

Both situations were compared with the behaviour of the cylindrical portion of the cladding, with the following loads and temperature conditions (see Fig. 7):

(a) A temperature gradient corresponding to the greatest power that the fuel can dissipate per unit length (687 watt/cm), and a temperature of 324 °C on the external surface of the cladding;
(b) An external constant pressure $P_{ext}$ on the cladding equal to that of the coolant (1·2 kg/mm$^2$);
(c) A variable pressure $P_{int}$ acting on the internal surface increasing from zero to the value causing the collapse of the cladding. This load is composed of the fission and initial filling gas pressures, and of the contact pressure

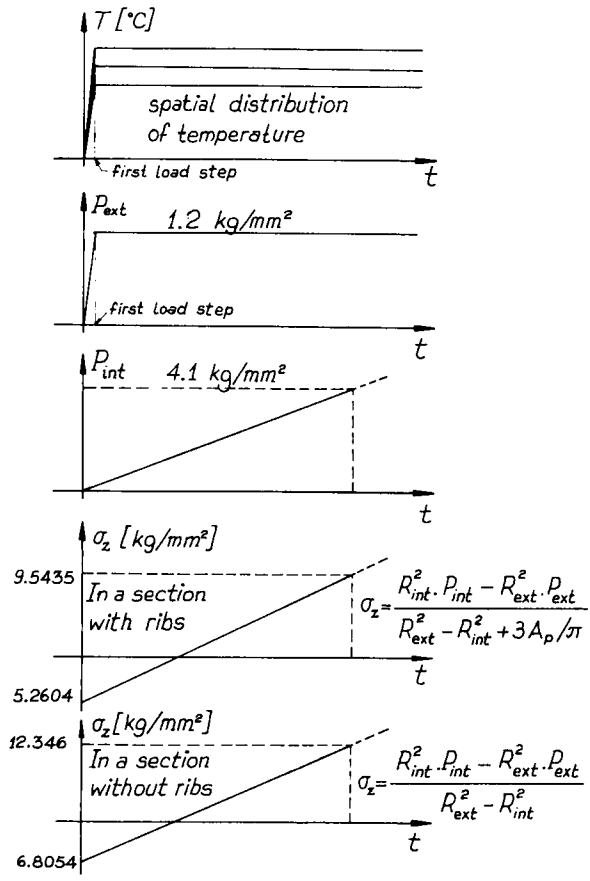


Fig. 7. Histories of stress, pressure and temperature for the reactor cladding.

between the pellets and cladding after the gap is closed. The gap closes due to thermal expansion and swelling of the fuel relative to the cladding.

(d) A longitudinal stress due to the simultaneous action of the internal and external pressures:

$$\sigma_z = \frac{R_{int}^2 \cdot P_{int} - R_{ext}^2 \cdot P_{ext}}{R_{ext}^2 - R_{int}^2 + 3A_p/\pi}$$

for the clad in the ribs zone ($A_p$ = area of each rib), and

$$\sigma_z = \frac{R_{int}^2 \cdot P_{int} - R_{ext}^2 \cdot P_{ext}}{R_{ext}^2 - R_{int}^2}$$

in the absence of ribs.

The thermal conductivities of each material have been taken as temperature dependent, according to the expressions given in ref. 7. For the Young's modulus of the cladding we adopt the value:

$$E = 10\,500 - 10T \text{ (kg/mm}^2\text{)}, \qquad T \text{ in °C}$$

and for the temperature dependence of the yield stress $\bar{\sigma}$ plotted in Fig. 8, we have:

$$\bar{\sigma} = H(\bar{\varepsilon}_p, T) = H(\bar{\varepsilon}_p, T_0) - 0{\cdot}0635(T - T_0) \text{ (kg/mm}^2\text{)}, \qquad T \text{ in °C}.$$

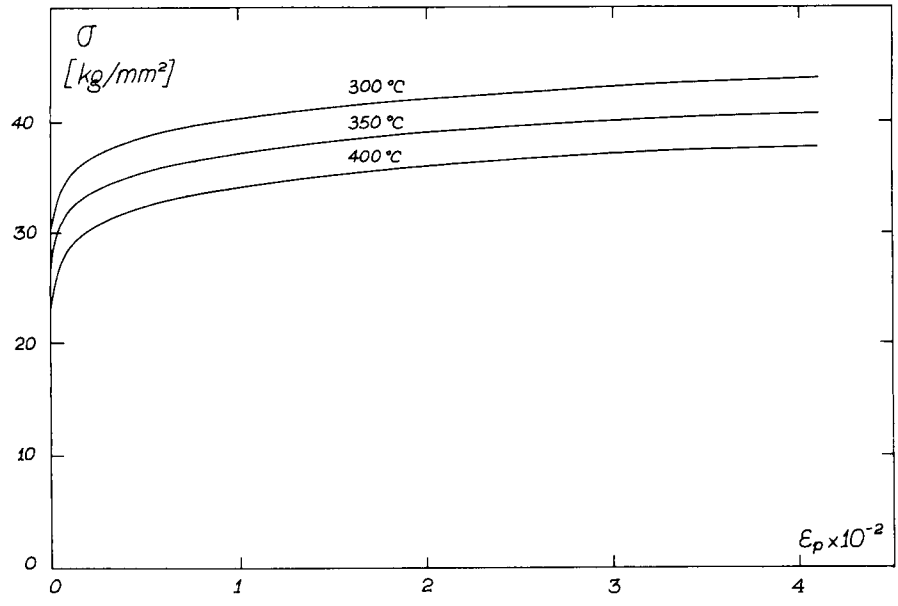


Fig. 8. Plot of $\bar{\sigma}$ versus $\bar{\varepsilon}_p$ for Zircaloy-4, at different temperatures.

The isotropic linear thermal expansion coefficient is $\alpha = 6{\cdot}5 \times 10^{-6}$ $(°C)^{-1}$, and the value of Poisson's ratio is $\nu = 0{\cdot}44$.

In case (i) we considered that the separator supports were absolutely rigid, i.e. they do not give under the pressure of expansion of the clad. This assumption was made because in a previous report[8] it was shown that the state of stress at the yield limit is practically unaffected by changing the stiffness constants of the separator.

4.3. *Description of the results and discussion*

The spatial distribution of temperature and the set of nodal loads representative of the pressures and longitudinal stress were calculated with the PREPLASTEF code. For reasons of symmetry, only a sector of 60° in Fig. 6 was considered. For the calculation of the temperature distribution in the ribbed cladding, the presence of the pellets was also included. In Fig. 6 the finite element mesh for the first case is also shown (only for the cladding), consisting of 218 nodes and 356 triangular elements. Without the ribs, the mesh employed is analogous, but with 126 nodes and 200 elements.

The thermoelastoplastic calculations were accomplished with the PLASTEF2 code, outlined in Section 2. For cases (i) and (ii) of Section 4.2, and for the cylindrical portion of the cladding, (a), (b) and (c) of Section 4.2 were incorporated in the first load step, with vanishing internal pressure $P_{int}$. Then, in the following load steps $P_{int}$ was increased according to the expected behaviour for each case. In Table 1 are shown the results for the following quantities:

(a) $P_y$: Internal pressure corresponding to the first yield.

TABLE 1.

VALUES OF $P_y$, $P_1$, $P_c$ AND THE ELASTIC AND PLASTIC WEAKENING COEFFICIENTS FOR THE THREE SITUATIONS ANALYSED (SEE TEXT FOR DEFINITIONS OF SYMBOLS)

| | *Clad in the ribs zone* | | |
|---|---|---|---|
| | *Without making contact with the separator* | *Initially in contact with a rigid separator* | *Clad cylindrical and infinite* |
| $P_y$ (kg/mm$^2$) | 3.30 | 2.10 | 3.70 |
| $P_1$ (kg/mm$^2$) | 3.84 | 3.90 | 3.92 |
| $P_c$ (kg/mm$^2$) | 4.04 | 4.00 | 4.13 |
| Elastic weakening coefficient: $P_y/P_y$ (cylin.) | 0.892 | 0.567 | 1.00 |
| Plastic weakening coefficient: $P_c/P_c$ (cylin.) | 0.98 | 0.97 | 1.00 |

(b) $P_1$: Internal pressure for which the two plastic enclaves, separately initiated at the internal and external surfaces of the cladding, make contact with each other (see Fig. 9).

(c) $P_c$: Internal pressure for which the cladding collapses.

In order to compare the different situations analysed, it will be necessary to define the *collapse internal pressure:* it is the internal pressure, greater than $P_1$, for which the relative radial displacement $u_r/r_{int}$ for a 'characteristic point' in the inner surface of the cladding attains a value of 2%. At this stage, the cladding has reached a state of stress almost entirely in the plastic range for the three different situations (see Figs. 9 and 11). In Table 1 are also shown the respective values of what we call 'the elastic and plastic weakening coefficients', that is, the ratios of $P_y$ and $P_c$ to the respective values ($P_y$ (cylin.) and $P_c$ (cylin.)) for the infinite cylindrical cladding.

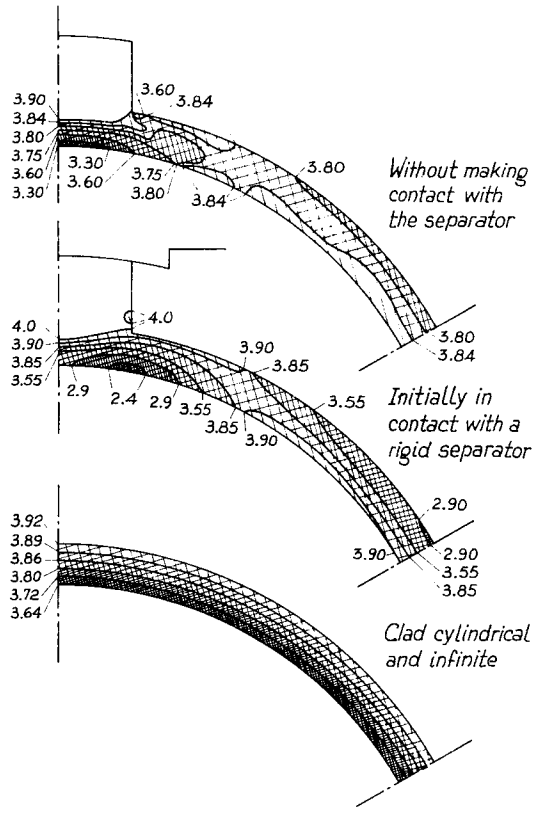


Fig. 9. Plastic enclaves for the different situations considered.

In Fig. 11 'characteristic points' B, B′ and B″ for the three cases are shown, and the displacements of these points are plotted against $P_{int}$. The corresponding values of $P_y$, $P_1$ and $P_c$ are shown. In small ranges of $P_{int}$ near the collapse, some lack of convergence in the algorithm was observed. These difficulties, in general, often appear during a sudden advance of the plastic zones, or when an advanced degree of plastification is reached (see for example refs. 1, 2, 5). They did not significantly affect the results here presented.

In Fig. 10 the original and the deformed geometry are shown (exaggerated), corresponding to an internal pressure $P_{int} = 3{\cdot}85\ kg/mm^2$ (near collapse). In Fig. 9 the plastic enclaves (that is, the portion of cladding in which all its points are in the plastic range), have been shown for successive values of $P_{int}$.

*Discussion*

As shown in Fig. 11 and Table 1, some critical point in the zone of the ribs reaches the yield stress for an internal pressure $P_{int}$ much smaller than for the

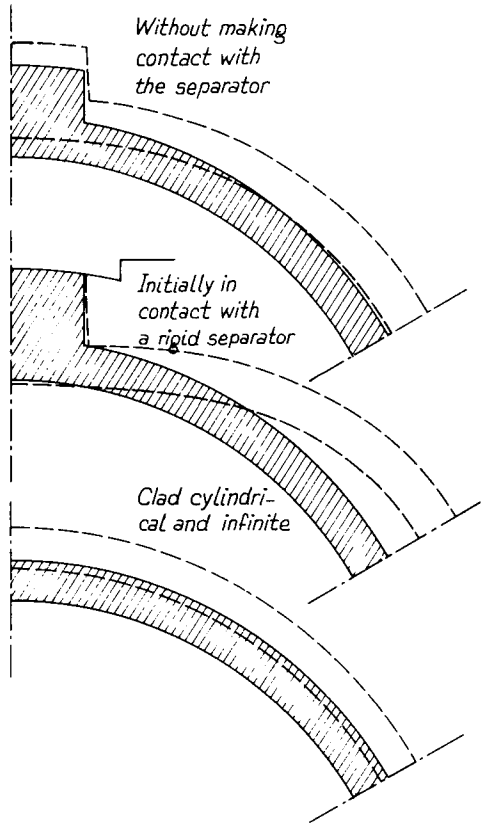


Fig. 10. Deformation patterns of the cladding.

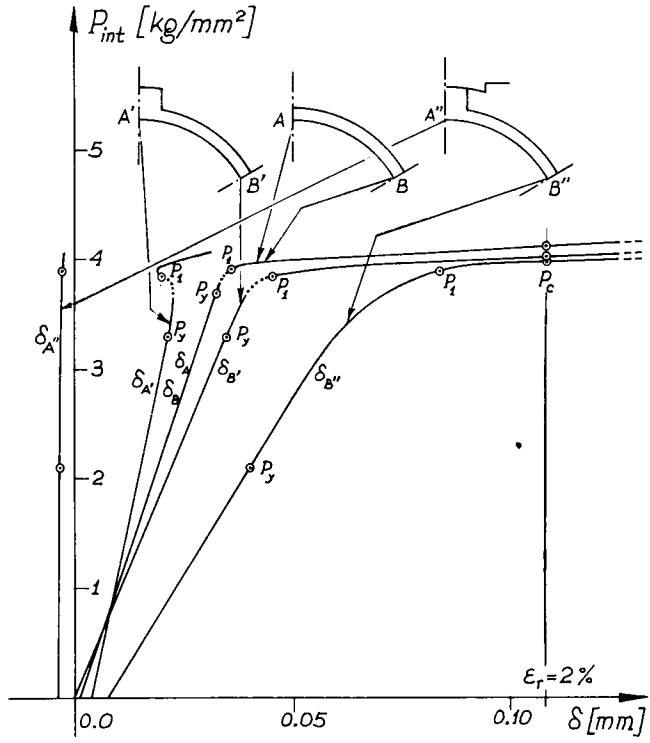


Fig. 11. Thermoelastoplastic displacement response of the reactor cladding at selected points, plotted against $P_{int}$.

cylindrical rib-free case. Nevertheless the collapse point is reached for practically the same values of $P_{int}$. From this fact a useful conclusion can be stated: *the slider ribs do not appreciably weaken the clad*, at least in elastoplastic collapse. This is in contrast to the conclusion one would obtain from a purely elastic study.[8]

Figure 11 discloses that the value of 2% for the strain, adopted in our definition of collapse internal pressure, does not have any significant effect on the values of the plastic weakening coefficients.

Though there are other important phenomena which influence the thermomechanical response of the cladding, such as creep, mechanical anisotropy, and radiation effects, it is plausible that when they are taken into account the same conclusion will still be drawn. The explanation is simple: the point of the cladding most stressed elastically is the first to reach the yield limit, and in its neighbourhood the material stays in a purely elastic state. These zones can continue absorbing the load increments while at the first point further plastic deformation takes place; here the state of stress remains almost unchanged. The

plastic 'enclave' grows and the initial region, where the stress concentration originated, finally becomes entirely plastic. This intuitive analysis explains how the ultimate collapse resistance of the cladding is almost that of an infinite cylinder.

For practical purposes, the collapse internal pressure is then almost the same, with or without ribs, with or without rigid separator supports. Nevertheless, observing carefully Fig. 11 and the values shown in Table 1, one notices that the order of increasing plastic weakness is: (1) infinite cylindrical clad; (2) clad with ribs but without making contact with the separator; (3) clad with ribs, always in contact with a rigid separator. This is just the expected behaviour.

## 5. CONCLUDING REMARKS

The tests described in Section 3 show a very satisfactory agreement with exact solutions and values obtained by other authors. These examples and others described in ref. 7 illustrate the trustworthiness of the codes. The greatest departures are observed for the values of the nodal averaged stresses. It is certain that they can be reduced considerably by employing more sophisticated elements than the constant stress triangles (the simplest ones) here used.

The application of one of the codes to the technological problem described in Section 4, has enabled us to draw valuable conclusions concerning the influence of the ribs on the collapse resistance of nuclear fuel element cladding.

The numerical experiments presented in ref. 5 and in this paper show the ability of the system PLASTEF to solve a great variety of two-dimensional thermoelastoplastic technological problems.

## ACKNOWLEDGMENTS

We wish to express our gratitude to Mr Neil Callwood for his patient revision of the manuscripts.

## REFERENCES

1. ZIENKIEWICZ, O. C., VALLIAPPAN, S. and KING, I. P., Elastoplastic solutions of engineering problems. Initial stress, finite element approach, *Int. J. Num. Meth. Engng*, **1** (1969) 75–100.
2. ZIENKIEWICZ, O. C., *The finite element method in engineering sciences*, London, McGraw Hill, 1971.
3. NAYAK, G. C. and ZIENKIEWICZ, O. C., Elasto-plastic stress analysis. A generalization for various constitutives relations including strain softening, *Int. J. Num. Meth. Engng*, **5** (1972) 113–35.

4. HILL, R., *The mathematical theory of plasticity*, Oxford, Clarendon Press, 1956.
5. BASOMBRÍO, F. G. and SÁNCHEZ SARMIENTO, G., PLASTEF: A code for the numerical simulation of thermoelastoplastic behaviour of materials using the finite element method, *N. Eng. Des.*, **46** (1978) 231–41.
6. BATHE, K. J., BOLOURCHI, S., RAMASWAMY, S. and SNYDER, M. D., Some computational capabilities for non linear finite element analysis, *N. Eng. Des.*, **46** (1978) 429–55.
7. SÁNCHEZ SARMIENTO, G. and BASOMBRÍO, F. G., *Finite element analysis of the Atucha Nuclear Reactor fuel cladding in the zone of the slider ribs* (in Spanish), CNEA-NT 6/79, 1979.
8. SÁNCHEZ SARMIENTO, G. and BASOMBRÍO, F. G., *Thermoelastic analysis of CNA type fuel element cladding on ribs zone and in contact with the separator* (in Spanish), CNEA report, 1979. (In press.)
9. HODGE, P. E. and WHITE, S. H., *J. Appl. Mech.* **17** (1950) 180.